PHYSICS AND CHEMISTRY
OF SOLID STATE
V. 27, No. 2 (2026) pp. 284-298

Section: Physics

DOI: 10.15330/pcss.27.2.284-298

*Vasyl Stefanyk Carpathian
National University*

ФІЗИКА І ХІМІЯ ТВЕРДОГО ТІЛА
Т. 27, № 2 (2026) С. 284-298

Фізико-математичні науки

PACS: 75.75.-c, 81.07.Bc, 82.50.Hp

ISSN 1729-4428 (Print)
ISSN 2309-8589 (Online)

J. Mazurenko[1,2,3], L. Turovska[4], M. Moklyak[5], L. Kaykan[1], V Moklyak[1,6]

Synthesis, Challenges, and Application Potential of Copper Ferrite Nanoparticles

[1]Laboratory for Physics of Magnetic Films, G.V. Kurdyumov Institute for Metal Physics, N.A.S. of Ukraine, Kyiv, Ukraine;
mazurenkoyus@nas.gov.ua, kaykan@nas.gov.ua
[2]Department of General Physics, Taras Shevchenko National University of Kyiv, Kyiv, Ukraine;
[3]Department of Medical Informatics, Medical and Biological Physics, Ivano-Frankivsk National Medical University, Ivano-Frankivsk, Ukraine;
[4]Department of Management and Business Administration, Faculty of Management, Vasyl Stefanyk Carpathian National University, Ivano-Frankivsk, Ukraine; liliia.turovska@cnu.edu.ua
[5]Department of Applied Physics and Materials Science, Vasyl Stefanyk Precarpathian National University, Ivano–Frankivsk, Ukraine; mariamoklyak@gmail.com
[5]Department of Physical and Mathematical Sciences, Ivano–Frankivsk National Technical University of Oil and Gas, Ivano–Frankivsk, Ukraine; volodymyr.mokliak@nung.edu.ua

Ferrites are ferrimagnetic iron-oxide–based materials whose magnetic and functional properties are governed by cation distribution, defects, and microstructure, all of which are strongly affected by synthesis. This review focuses on spinel copper ferrite ($CuFe_2O_4$) nanoparticles, emphasizing how synthesis-controlled structure determines multifunctional performance. Particular attention is given to the coexistence and stabilization of tetragonal and cubic $CuFe_2O_4$ phases, the role of Jahn–Teller distortion of Cu^{2+}, and the influence of oxygen nonstoichiometry, cation redistribution, and surface disorder in the nanoscale regime. The most widely used chemical routes – co-precipitation, hydrothermal/solvothermal synthesis, and sol–gel (including autocombustion) – are discussed with respect to their ability to control phase purity, crystallinity, particle size, morphology, and defect chemistry. The structure–property framework is then linked to key application domains covered in this work: visible-light-driven photocatalytic degradation of dyes, adsorption-based removal of pollutants, photocatalytic hydrogen evolution, electromagnetic interference shielding/microwave attenuation, and functional sensing platforms. Finally, practical limitations are summarized, including reproducibility of cation/defect states, phase stability, performance degradation, and regeneration, highlighting the need for standardized evaluation protocols and rational materials design for scalable, reusable $CuFe_2O_4$-based technologies.

Keywords: Spinel ferrites; Copper ferrite nanoparticles; Water purification; Photocatalysis; EMI shielding; Magnetic recovery and reuse; Green synthesis.

Received 14 November 2026; Accepted 02 May 2026; Published 03 June 2026.

Content

Introduction

Ferrites [1] are a class of ferrimagnetic materials composed primarily of complex iron (III) oxide–based compounds, exhibiting magnetic behavior due to superexchange interactions between metal cations mediated by oxygen anions in a crystalline lattice. These materials derive their magnetism from the antiparallel alignment of magnetic moments on tetrahedral (A) and octahedral (B) sites within the lattice, leading to a net magnetization characteristic of ferrimagnetism. Based on their crystallographic structures and the molar ratio of Fe_2O_3 to other metal oxides, ferrites are categorized into four main groups: spinel ferrites, garnets, orthoferrites, and hexaferrites. Each subclass exhibits distinctive structural, magnetic, and electronic properties, which support their diverse applications.

Among these, spinel ferrites – with the general formula MFe_2O_4 (where M is a divalent metal cation such as Cu^{2+}, Ni^{2+}, Co^{2+}, etc.) – are particularly prominent due to their structural versatility, chemical stability, mechanical hardness, and electromagnetic properties. The spinel structure, characterized by a cubic close–packed arrangement of oxygen anions and metal cations distributed over tetrahedral and octahedral interstices, allows for significant tunability of physical properties through cation substitution or redistribution. This adaptability makes spinel ferrites highly suitable for applications in magnetic storage, catalysis, microwave absorption, gas sensing, and biomedicine.

Notably, the properties and technological utility of ferrites are not solely determined by their stoichiometric composition but are strongly influenced by the synthesis method [2], which affects factors such as crystallite size, morphology, cation distribution, and defect density. A wide array of synthesis techniques – including sol–gel, co–precipitation, hydrothermal, microwave–assisted, and mechanochemical methods – have been developed to tailor the microstructure and magnetic properties of ferrites for specific applications.

Among spinel ferrites, copper ferrite ($CuFe_2O_4$) nanoparticles stand out as versatile and promising materials due to their tuneable magnetic, electronic, catalytic, and structural properties. The unique physicochemical characteristics of $CuFe_2O_4$ can be modulated by varying synthesis conditions and external stimuli, making them adaptable for a wide range of technological applications [3–5].

Owing to this multifunctionality, $CuFe_2O_4$ nanoparticles have attracted significant interest across various fields. They have been employed as anode materials in lithium–ion batteries [6], contrast agents for magnetic resonance imaging (MRI) [7], and photocatalysts for hydrogen evolution under visible light irradiation [8]. Additionally, they serve as electrocatalysts for CO_2 reduction [9], catalysts for organic coupling reactions [10], photoanodes for solar water splitting [11], supports for enzyme immobilization [12], and materials for nanomedicine applications including cancer therapy [13].

Structurally, $CuFe_2O_4$ exhibits two crystallographic phases: a tetragonal phase (stable at room temperature) and a metastable cubic phase (which can be stabilized under specific synthesis conditions). The coexistence or selective stabilization of these phases significantly influences the material's magnetic anisotropy, electronic band structure, and catalytic activity.

At room temperature, $CuFe_2O_4$ typically crystallizes in a tetragonal spinel structure (fig. 1(a)), which represents its stable low–temperature phase, while a metastable cubic phase (fig. 1(b)) can be stabilized at high temperatures or under specific synthesis conditions. The preference for the tetragonal structure arises from the electronic configuration of Cu^{2+} cations, which tend to occupy octahedral (B) sites due to their ability to form covalent bonds within complex ions. The presence of Cu^{2+} ions, characterized by a Jahn – Teller–active d^9 electronic configuration [15], induces a significant distortion of the octahedral coordination environment, leading to a pronounced tetragonal elongation (c/a > 1.1).

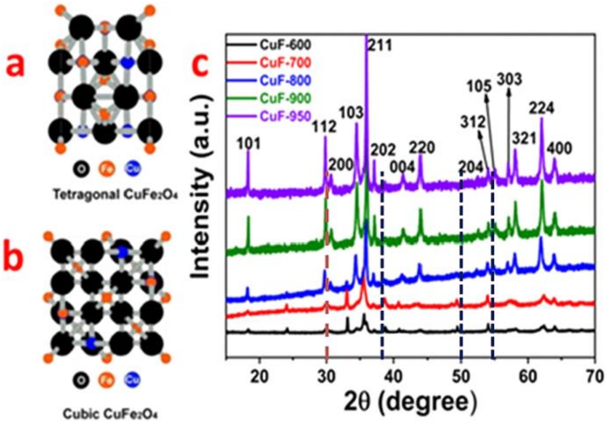

Fig. 1. Crystal structure of $CuFe_2O_4$ (a) typical structure (tetragonal), (b) inverse spinel ferrite (cubic), and (c) XRD patterns of spinel–type $CuFe_2O_4$ photocatalysts.

Adapted from [14].Upon heating, thermal excitation weakens the covalent Cu – O bonds in planes perpendicular to the c–axis, facilitating a tetragonal–to–cubic phase transition as the cooperative Jahn – Teller distortion diminishes. The Jahn – Teller effect in $CuFe_2O_4$ has been experimentally investigated using single–crystal synchrotron X–ray diffraction under high pressure. Kyono et al. [16] demonstrated that increasing pressure progressively reduces the distortion around the Cu^{2+} ions, with the coordination polyhedra approaching a regular octahedral geometry. At a critical pressure of 4.6 GPa, a cubic–to–tetragonal transition occurs, evidenced by the splitting of the cubic lattice parameter into distinct *a* and *c* axes (a = 5.882 Å, c = 8.337 Å). This structural evolution reflects an increase in electrostatic repulsion between the oxygen ligands and the $3d(z^2)$ orbital of the Cu^{2+} ion.

Complementary studies have also explored temperature–driven structural transformations in $CuFe_2O_4$. Nedkov et al. [17] suggested that the tetragonal–to–cubic transition may be partially governed by oxygen nonstoichiometry and the formation of Cu^+ ions in the lattice, implying a coupling between redox behaviour and structural rearrangement. Supporting this, Kester et al. [18] provided thermodynamic evidence that reduction reactions during thermal treatments or quenching can increase the fraction of Cu^+ at octahedral sites, affecting both the phase stability and the material's magnetic properties.

The synthesis route plays a crucial role in controlling these structural features. Studies on nanoscale $CuFe_2O_4$ particles (10 – 30 nm) have shown that high–temperature processing can induce surface structural and magnetic disorder, resulting in deviations from bulk–like behaviour. Jiang et al. [19] and others reported that such disorders may arise from cation redistribution, oxygen vacancies, amorphization, and the formation of structurally distinct surface layers. These factors collectively complicate the interpretation of structure – property correlations in nanosized copper ferrite.

Therefore, both intrinsic factors – such as cation electronic configuration and Jahn – Teller distortions – and extrinsic factors – including synthesis method, particle size, thermal treatment, and defect chemistry – must be considered to fully understand and optimize the physicochemical properties of $CuFe_2O_4$. The interplay of these parameters necessitates precise control over synthesis conditions to achieve materials with reproducible structures and targeted functionalities for their intended applications.

I. Chemical Synthetic Strategies and Their Impact on Structure–Property Relationships

A variety of chemical synthesis methods have been developed for the preparation of nanosized spinel ferrites, including copper ferrite ($CuFe_2O_4$). Among these, co-precipitation, sol–gel–based approaches, and hydrothermal/solvothermal synthesis dominate the $CuFe_2O_4$ literature, as they provide the most direct and reproducible control over phase composition, crystallinity, particle size, and defect chemistry-parameters that critically govern magnetic and functional properties.

The co-precipitation method represents a simple and scalable route for producing nanocrystalline $CuFe_2O_4$ with tunable stoichiometry and magnetic behavior, though it often yields defect-rich and agglomerated particles [20, 21]. In contrast, sol–gel synthesis, particularly when combined with self-combustion (autocombustion), enables molecular-level mixing of precursors, resulting in chemically homogeneous powders and improved control over crystallite size and phase formation at relatively low calcination temperatures [22–24]. This approach is especially effective for doped and substituted $CuFe_2O_4$ systems.

Hydrothermal and solvothermal methods offer enhanced control over crystallinity and morphology by promoting direct crystallization under elevated temperature and pressure, often without the need for high-temperature post-annealing [20]. These methods are particularly valuable for stabilizing metastable phases and for disentangling intrinsic lattice effects from surface disorder.

Other synthesis routes-such as solid-state reactions, microemulsion techniques, mechanochemical processing, or high-energy milling-have been reported for $CuFe_2O_4$ preparation [25–32]. However, their limited scalability, reproducibility, or control over structure–property relationships restrict their relevance for systematic comparison and are therefore not discussed in detail here.

Overall, the selection of synthesis route plays a decisive role in determining the structural, magnetic, and functional characteristics of $CuFe_2O_4$ nanoparticles, making rational method choice essential for targeted environmental and catalytic applications.

1.1. Co-precipitation and precipitation-derived approaches.

The co-precipitation method is widely recognized as a simple, scalable, and economically viable route for synthesizing spinel-type magnetic nanoparticles, including $CuFe_2O_4$. This wet-chemical approach enables the formation of structurally homogeneous ferrite nanoparticles with tunable crystallite size and magnetic properties [33].

Typically, stoichiometric solutions of metal precursors-such as chlorides, nitrates, or sulfates of Cu^{2+} and Fe^{3+}-are reacted with a basic precipitating agent (e.g., NaOH, KOH, or NH_4OH) under controlled temperature and pH conditions. Key synthesis parameters, including reaction temperature, pH, aging time, and metal ion ratio, strongly influence particle size, crystallinity, cation distribution, and magnetic behavior of the resulting $CuFe_2O_4$ nanoparticles [34, 35]. After precipitation, the hydroxide precursors are washed, dried, and thermally treated to obtain the spinel $CuFe_2O_4$ phase [36].

A major advantage of co-precipitation lies in its industrial relevance, as it can be readily scaled to kilogram-level production while maintaining acceptable compositional accuracy [37,38]. For $CuFe_2O_4$, this method typically yields nanoparticles in the 10–25 nm size range; however, broad size distributions and strong agglomeration are commonly observed due to magnetic dipole interactions. As a result, saturation magnetization values are often lower than those of bulk materials, reflecting cation disorder and surface spin canting. At the same time, the high density of surface defects and oxygen vacancies can enhance photocatalytic and adsorptive activity. Indeed, co-precipitated $CuFe_2O_4$ has demonstrated efficient visible-light-driven degradation of organic dyes such as methylene blue and rhodamine B [39–41], with representative particle sizes of 16–26 nm shown in Figure 2 [40,41].

Compared to sol–gel and hydrothermal synthesis, co-precipitation offers limited control over particle morphology and size uniformity and generally requires post-synthesis calcination, which may induce grain growth or secondary phase formation (e.g., CuO or Fe_2O_3). Nevertheless, its simplicity, low cost, and scalability make co-precipitation particularly attractive for environmental applications. Future optimization should focus on suppressing agglomeration, improving crystallinity at lower temperatures, and enhancing morphology control through polymer-assisted precipitation, templating strategies, or in situ surface functionalization.

1.2. Hydrothermal and Solvothermal Synthesis Methods.

Hydrothermal and solvothermal synthesis routes are among the most effective wet-chemical methods for producing highly crystalline spinel ferrite nanoparticles, including $CuFe_2O_4$, with controlled particle size and morphology. In solvothermal synthesis, metal precursors are dissolved in non-aqueous solvents such as ethanol or ethylene glycol and reacted at elevated temperatures under autogenous pressure, enabling controlled nucleation and growth. In contrast, hydrothermal synthesis is carried out in aqueous media at temperatures above the boiling point of water in sealed autoclaves, providing enhanced control over crystallinity, particle size, and phase purity [42].

As illustrated schematically in Figure 3, hydrothermal processing enables direct crystallization of ferrite nanoparticles without the need for high-temperature post-annealing [43]. The combined effect of elevated temperature and pressure suppresses structural disorder, promotes single-crystal growth, and facilitates improved cation ordering within the spinel lattice. These conditions are particularly advantageous for stabilizing metastable phases and minimizing surface defect density, allowing intrinsic structure–property relationships to be more clearly resolved.

Hydrothermal and solvothermal methods also allow access to a wide range of particle morphologies, including nanocubes, hollow spheres, and hierarchical nanostructures, which are difficult to obtain using conventional precipitation techniques [44–46]. Among the synthesis parameters, reaction temperature plays a

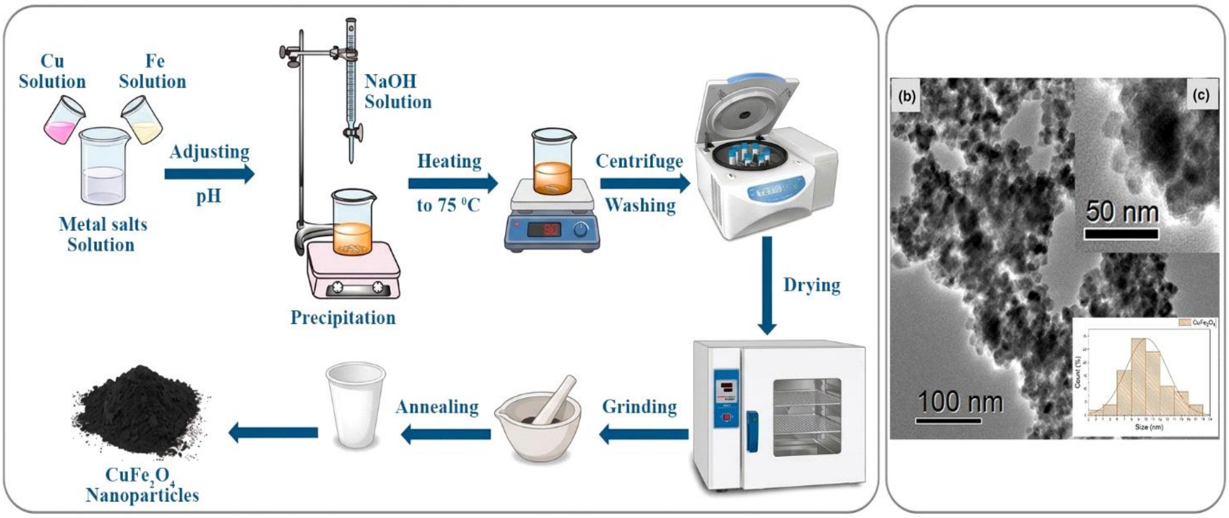

Fig. 2. (a) Schematic representation of the co–precipitation synthesis route for $CuFe_2O_4$ nanoparticles, (b) TEM micrograph illustrating particle morphology, and (c) HRTEM image revealing the crystalline structure of $CuFe_2O_4$ nanoparticles. Adapted from [41].

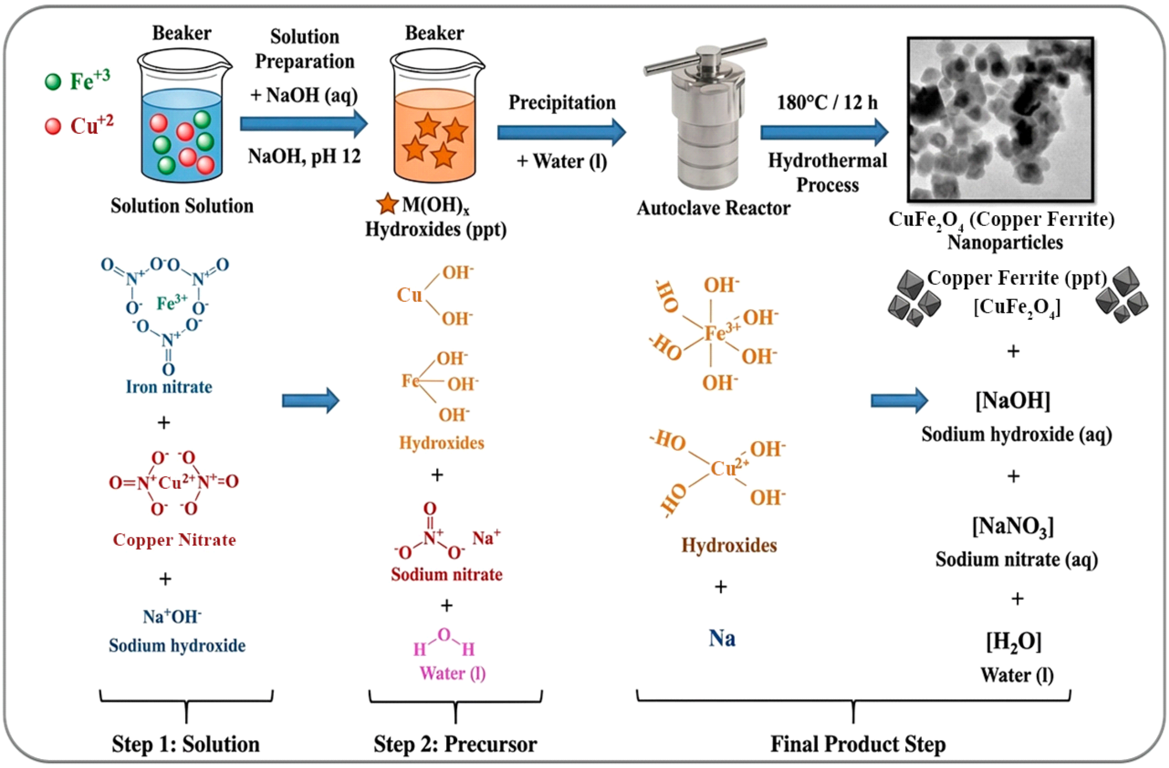

Fig. 3. Schematic illustration of the hydrothermal synthesis process. Adapted from [43].

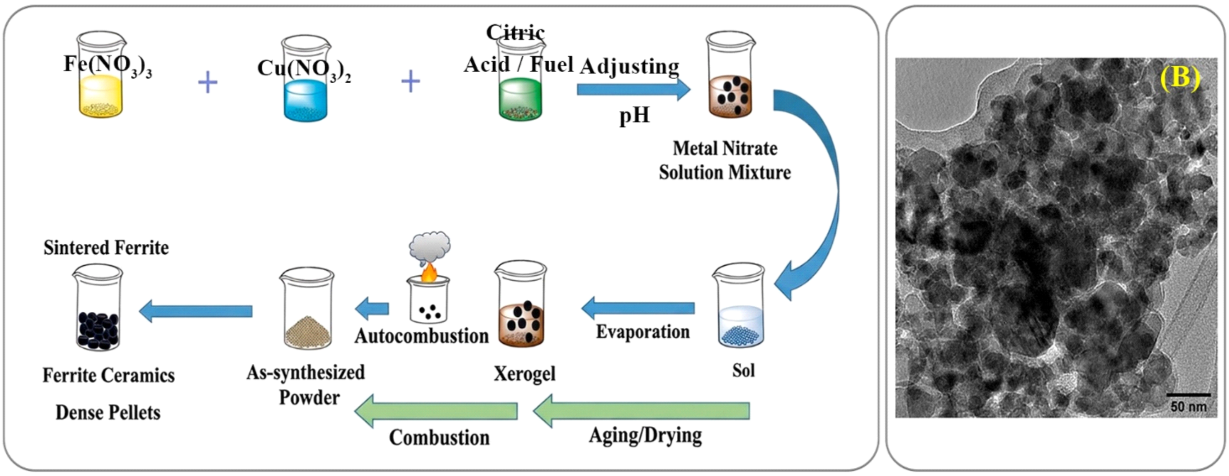

Fig. 4. (a) Schematic illustration of the synthesis of spinel ferrite and transition metal–substituted spinel ferrite nanoparticles using the sol–gel method [Adapted from 53, 54]; (b) $CuFe_2O_4$ nanoparticles synthesized by the sol–gel technique [Adapted from 55].

dominant role, governing nucleation kinetics, crystal growth rates, and final particle morphology, while reaction time and precursor concentration provide additional tuning of crystallite size and surface characteristics [44, 47].

Owing to their high degree of tunability, hydrothermal and solvothermal routes are particularly valuable for the synthesis of phase-pure, well-crystallized $CuFe_2O_4$ and related composites, such as $CuFe_2O_4/SiO_2$ systems (Figure 4), where controlled crystallinity and interfacial structure are essential for catalytic and environmental applications [43, 48]. However, the need for sealed high-pressure reactors and relatively long reaction times may limit large-scale implementation compared to simpler precipitation-based methods.

1.3. Sol–gel combustion/autocombustion methods

Sol–gel synthesis is one of the most widely employed chemical routes for preparing $CuFe_2O_4$ nanoparticles when high compositional homogeneity and precise control over crystallite size and phase formation are required. In this approach, metal precursors-typically nitrates or acetates of Cu and Fe-are hydrolyzed and condensed in solution to form a homogeneous gel, which upon drying and calcination yields crystalline $CuFe_2O_4$. Owing to molecular-level mixing of cations, sol–gel processing is particularly effective for doped and substituted $CuFe_2O_4$ systems, where stoichiometric control and uniform cation distribution are critical for tuning magnetic and electronic properties [49-52].

A notable variant of this method is sol–gel autocombustion, which couples gel formation with a self-sustaining redox reaction between metal nitrates and an organic fuel such as citric acid, glycine, or urea. During ignition, the xerogel undergoes rapid exothermic combustion, generating sufficient thermal energy for in situ crystallization of the spinel phase without prolonged high-temperature annealing. The combustion temperature, typically in the range of 600–1350 °C, depends strongly on the fuel-to-oxidizer ratio and precursor chemistry [27, 56-58].

Sol–gel autocombustion offers several advantages over conventional sol–gel processing, including higher phase purity, reduced processing time, and improved chemical homogeneity. By adjusting parameters such as pH, fuel content, and heating rate, it is possible to tailor crystallite size, defect concentration, and morphology, enabling the synthesis of $CuFe_2O_4$ nanospheres, porous aggregates, or anisotropic nanostructures [59]. For example, $CuFe_2O_4$ nanoparticles synthesized via autocombustion typically exhibit uniform morphology with average particle sizes on the order of several tens of nanometers, while standard sol–gel routes can yield broader size distributions depending on calcination conditions [60, 61].

Despite these advantages, sol–gel–based methods often require careful control of processing parameters to avoid secondary phase formation or excessive grain growth during calcination. Nevertheless, their versatility, reproducibility, and suitability for compositional engineering make sol–gel and sol–gel autocombustion methods central to systematic studies of structure–property relationships in $CuFe_2O_4$, particularly for photocatalytic and magnetic applications.

II. Functional Applications of Copper Ferrite Nanoparticles and Nanocomposite

The tunable structural, electronic, and magnetic properties of copper ferrite ($CuFe_2O_4$) nanoparticles have enabled their exploration across a wide range of technological applications. Control over particle size, crystallinity, morphology, and surface chemistry through chemical synthesis routes has facilitated the use of $CuFe_2O_4$ in energy storage, catalysis, biomedicine, and environmental remediation.

$CuFe_2O_4$ has been investigated as an anode material for lithium-ion batteries and as an electrode or electrocatalyst in energy conversion systems, owing to its mixed-valence states and redox activity [62, 63, 64]. In addition, its magnetic response and biocompatibility have motivated studies in biomedical fields, including magnetic targeting and imaging-related applications [52, 65, 66]. However, many of these applications remain limited to

Table 1.

Summary of photocatalytic activity on $CuFe_2O_4$ spinel ferrites.

Photocatalyst	Pollutant	Experimental Conditions	Findings	Ref.
$CuFe_2O_4$	MG	Visible light (75W); 0.2 g · L^{-1} catalyst; 20 ppm dye; 60 min	~56.60 % deg.	[68]
$CuFe_2O_4$	RhB	Visible light (75W); 0.4 g · L^{-1} catalyst; 5 ppm dye; 60 min	~84.30 % deg.	[68]
$CuFe_2O_4$	DR 264	Visible light (Xenon); 2.0 g · L^{-1} catalyst; 10 mL H_2O_2 (0.1M); 80 ppm dye; 120 min	~94.76 % deg.	[71]
$CuFe_2O_4$	MB	Mercury lamp (260 W); 0.2 g · L^{-1} catalyst; 30 mg· L^{-1} dye; pH 9; 130 min	~94.2 % deg.	[72]
$CuFe_2O_4$ (hydrothermal)	MB	Visible light (Solar simulation 50mW/cm^2); 10 mg catalyst; 0.05% dye solution; 120 min	~55 % deg;	[73]
$CuFe_2O_4$ (coprecipitation)	MB	Visible light (Solar simulation 50mW/cm^2); 10 mg catalyst; 0.05% dye solution; 120 min	~35 % deg;	[73]
$CuFe_2O_4$ (sol-gel)	MB	Visible light (Solar simulation 50mW/cm^2); 10 mg catalyst; 0.05% dye solution; 120 min	~42 % deg;	[73]
La-doped $CuFe_2O_4$	FOR	Sunlight; 0.4 g · L^{-1} catalyst; 20 ppm dye; 90 min	~91.7 % deg;	[74]

deg. – degradation; MG – Malachite Green; RhB – Rhodamine B; DR-264 – Direct Red 264; MB – Methylene Blue; FOR – Fast Orange Red.

laboratory-scale demonstrations and are strongly dependent on precise control of phase purity and surface chemistry.

Among the various application domains, environmental and catalytic uses of $CuFe_2O_4$ nanoparticles have attracted particular attention. Their narrow band gap, visible-light activity, high surface area, and magnetic recoverability make them especially suitable for photocatalytic hydrogen evolution and degradation of organic pollutants under solar or visible light irradiation [67, 68, 69]. These properties, combined with low material cost and chemical stability, position $CuFe_2O_4$-based nanomaterials as promising candidates for sustainable environmental remediation technologies.

Accordingly, the following sections focus on the photocatalytic and environmental applications of $CuFe_2O_4$ nanoparticles and nanocomposites, with emphasis on structure–property relationships governing catalytic performance and reusability.

2.1. Photocatalytic decomposition of dyes

Synthetic dyes are widely used as model pollutants in photocatalytic studies due to their strong optical absorption and persistence in aquatic environments, particularly in textile wastewater. Their degradation can be conveniently monitored by UV–visible spectroscopy, and reaction kinetics are often described using the Langmuir–Hinshelwood model [68, 70].

$CuFe_2O_4$ nanoparticles and their composites have demonstrated effective visible-light-driven degradation of a broad range of dyes, including Methylene Blue, Rhodamine B, Congo Red, and Orange II. Representative studies summarizing degradation efficiencies, reaction conditions, and catalyst compositions are compiled in Table 1.

Although pristine $CuFe_2O_4$ exhibits moderate photocatalytic activity, performance can be significantly enhanced through heterojunction formation, oxidant-assisted processes (e.g., H_2O_2-activated Fenton-like reactions), or optimized irradiation conditions. Comparative studies indicate that while TiO_2 and ZnO remain superior under UV light, $CuFe_2O_4$ outperforms these wide-band-gap materials under visible-light irradiation and offers superior long-term stability and recyclability [68, 71-74].

2.2. Adsorption-based pollutant removal

Adsorption is a widely applied and energy-efficient approach for wastewater treatment, particularly suitable for the removal of dyes, heavy metals, and emerging contaminants from complex aqueous matrices. In recent years, magnetic nanoadsorbents have attracted increasing attention due to their ease of separation and reusability, with copper ferrite ($CuFe_2O_4$) nanoparticles emerging as promising candidates.

$CuFe_2O_4$ exhibits several features desirable for adsorption-based remediation, including moderate-to-high surface area, chemical stability, low synthesis cost, and superparamagnetic behavior that enables rapid magnetic separation after treatment. In addition, the surface of $CuFe_2O_4$ nanoparticles can be readily functionalized with polymers, organic ligands, or inorganic phases, allowing tailored interactions with target pollutants via electrostatic attraction, hydrogen bonding, π–π interactions, or surface complexation.

While pristine $CuFe_2O_4$ shows moderate adsorption capability, its performance is often significantly enhanced through composite formation. Hybrid materials such as $CuFe_2O_4$@g-C_3N_4 and polymer-modified $CuFe_2O_4$ have demonstrated improved adsorption capacity and selectivity toward organic dyes, pharmaceuticals, and inorganic contaminants, attributed to increased surface area, improved dispersibility, and synergistic interfacial effects [75-78]. In many cases, adsorption serves as a pre-concentration step that facilitates subsequent photocatalytic degradation under light irradiation.

$CuFe_2O_4$-based nanoparticles and nanocomposites have been extensively investigated for the removal of toxic metal ions, including Hg^{2+}, Cr^{6+}, As^{3+}, Cd^{2+}, Pb^{2+}, Mn^{2+}, and Ni^{2+}, owing to their magnetic recoverability, tunable surface chemistry, and redox-active sites. Representative findings are summarized in Table 2, confirming the potential of $CuFe_2O_4$ nanostructures as recyclable and environmentally friendly adsorbents.

Although no universal optimum pH exists, most studies report maximum adsorption near the point of zero charge (pH ≈ 3.7–8.1), indicating the dominant role of electrostatic attraction and surface complexation. Adsorption behavior generally follows Langmuir isotherms and pseudo-second-order kinetics, suggesting monolayer chemisorption as the prevailing mechanism. Surface modification using biopolymers, carbonaceous supports, or metal–organic frameworks further enhance adsorption capacity and selectivity, underscoring the importance of surface engineering for targeted metal removal.

2.3. Hydrogen evolution reaction in water–splitting processes

Photocatalytic water splitting represents a sustainable approach for hydrogen production using solar energy, particularly under visible-light irradiation. In this process, semiconductor photocatalysts generate photogenerated charge carriers that drive hydrogen evolution reactions at the catalyst surface.

Copper ferrite nanoparticles ($CuFe_2O_4$ NPs) have attracted increasing attention as visible-light-active photocatalysts for hydrogen evolution owing to their narrow band gap (approximately 1.7–1.9 eV), favorable band alignment, and intrinsic Cu^{2+}/Cu^{+} and Fe^{3+}/Fe^{2+} redox couples, which promote interfacial charge transfer. In addition, $CuFe_2O_4$ exhibits good photochemical stability, low toxicity, and cost effectiveness, making it attractive for sustainable energy applications.

Photocatalytic hydrogen production using $CuFe_2O_4$ has been investigated in both sacrificial reagent-assisted systems and pure water splitting configurations. Numerous studies have demonstrated that hydrogen evolution rates can be significantly enhanced through the formation of heterostructures or nanocomposites with secondary semiconductors or conductive supports, which suppress electron–hole recombination and improve

Table 2.

Performance of various $CuFe_2O_4$-based composites and doped nanoferrites for the removal of heavy metal ions from aqueous solutions.

Catalyst	Pollutant	Experimental Conditions	Findings	Ref.
$CuFe_2O_4$ / Sepiolite / GO	Pb (II)	Batch adsorption; 1.0 g · L^{-1}; pH 6; 298K	208.33 mg · g^{-1} (max capacity)	[79]
$CuFe_2O_4$ / Sepiolite / GO	Cd (II)	Batch adsorption; 1.0 g · L^{-1}; pH 6; 298K	147.02 mg · g^{-1} (max capacity)	[79]
$CuFe_2O_4$ @ PTh	Hg (II)	Batch adsorption; 1.0 g; pH 7; 298K; 60 min	90 mg · g^{-1} (max capacity)	[80]
$CuFe_2O_4$	Hg (II)	Batch adsorption; 1.0 g; pH 7; 298K; 60 min	35 mg · g^{-1} (max capacity)	[80]
$CuFe_2O_4$	Pb (II)	Dosage 0.1 g; pH 6; 120 min	~78 % removal	[81]
Zn- $CuFe_2O_4$	Pb (II)	Dosage 0.1 g; pH 6; 120 min	~98.5 % removal	[81]
Co- $CuFe_2O_4$	Pb (II)	Dosage 0.1 g; pH 6; 120 min	~91.5 % removal	[81]
Zn- $CuFe_2O_4$	Cd (II)	Dosage 0.1 g; pH 6; 120 min	~95.5 % removal	[81]
$CuFe_2O_4$ / $ZnIn_2S_4$	Cr (VI)	Simulated sunlight; 0.4 g · L^{-1} catalyst; 10 mg · L^{-1} Cr (VI); 120 min	~98.2 % removal	[82]
$CuFe_2O_4$	Cr (VI)	Simulated sunlight; 0.4 g · L^{-1} catalyst; 10 mg · L^{-1} Cr (VI); 120 min	~20 % removal	[82]

GO – Graphene Oxide; PTh - Polythiophene

Table 3.

Performance of various $CuFe_2O_4$-based composites and doped nanoferrites for the hydrogen evolution from water splitting.

Electrocatalyst	Experimental Conditions	Findings	Ref.
$CuFe_2O_4$	1.0 M KOH electrolyte; Glassy carbon electrode; 298 K	Overpotential: 253 mV (at 10 mA · cm^{-2}); Tafel slope: 118 mV · dec^{-1}	[83]
$CuFe_2O_4$/PANI	1.0 M KOH electrolyte; Hydrothermal synthesis; Room temperature	Overpotential: 194 mV (at 10 mA · cm^{-2}); Tafel slope: 34 mV · dec^{-1}; Stability: 30 h; Onset potential: 1.39 V	[63]
$CuFe_2O_4$	1.0 M KOH electrolyte; Co-precipitation method; HER application	Onset potential: 0.247 V vs. RHE; Tafel slope: 85 mV · dec^{-1}; H_2 generation rate: 1072.9 μmol · h^{-1}	[83]
$CuFe_2O_4$/TCPP (Porphyrin)	PEC Water Splitting; FTO substrate; Simulated sunlight; 0.1 M Na2SO4	Current density: 6.94 mA · cm^{-1} (at 1.23 V vs. RHE); Resistance dropped from 33.8 kΩ to 4.1 kΩ under light	[84]
BiVO4/$CuFe_2O_4$	PEC Water Splitting; FTO substrate; 0.5 M Na2SO4	Photocurrent: 2.77 mA · cm^{-2}; Charge separation efficiency: 79.7%	[11]
$CuFe_2O_4$/CuO	PEC Water Splitting; Spray pyrolysis; FTO substrate; 0.1 M Na_2SO_4	Photocurrent: 17 μA/cm^2 (@ 0.7 V vs. RHE); 2.6-fold increase over pure $CuFe_2O_4$	[85]

PANI – Polyaniline; HER - Hydrogen Evolution Reaction; RHE - Reversible Hydrogen Electrode; TCPP - Tetrakis(4-carboxyphenyl) porphyrin; PEC - photo-electrochemical; FTO substrate - Fluorine-doped Tin Oxide;

visible-light absorption. Representative studies summarizing synthesis routes, composite architectures, and hydrogen evolution performance are compiled in Table 3.

The photocatalytic activity of $CuFe_2O_4$-based systems is strongly influenced by synthesis-induced microstructural features such as crystallinity, surface area, and defect concentration, as well as by experimental parameters including pH, catalyst loading, and irradiation conditions. Rational design of heterojunction or Z-scheme architectures with materials such as TiO_2 or g-C_3N_4 further enhances charge separation and redox efficiency.

Although the hydrogen evolution activity of $CuFe_2O_4$ remains lower than that of state-of-the-art noble-metal-based photocatalysts, its visible-light response, environmental compatibility, and magnetic recoverability make $CuFe_2O_4$-based nanocomposites promising candidates for scalable and recyclable solar hydrogen production systems.

2.4. Electromagnetic Interference Shielding Performance of $CuFe_2O_4$-Based Nanomaterials

Electromagnetic interference (EMI) shielding materials attenuate incident electromagnetic radiation primarily through reflection (impedance mismatch and free-charge carrier response) and absorption (dielectric/magnetic losses and interfacial polarization). In practical reporting, shielding performance is commonly quantified by the total shielding effectiveness (SE_T, dB) and its components SE_R and SE_A, while absorber-oriented studies frequently report reflection loss (R_L, dB) and effective absorption bandwidth (EAB, $R_L < -10$ dB). Recent reviews emphasize that modern EMI solutions increasingly aim for absorption-dominant shielding to mitigate secondary reflection pollution and improve stealth/compatibility with nearby electronics. [86-88].

CuFe2O4 (copper ferrite) contributes to shielding/absorption via several coupled mechanisms [89, 90]:

Magnetic losses in $CuFe_2O_4$-based materials mainly originate from natural and exchange resonance processes, accompanied by frequency-dependent permeability dispersion, while eddy-current losses may also contribute depending on the electrical conductivity and characteristic particle size. Dielectric losses arise primarily from dipolar relaxation and defect-induced polarization phenomena, with electron hopping processes (such as Fe^{2+}/Fe^{3+} transitions) further enhancing dielectric dissipation and electromagnetic attenuation. Interfacial polarization plays a significant role in nanostructured composites, where the presence of abundant interfaces in ferrite–polymer, ferrite–carbon, and ferrite–sulfide systems promotes Maxwell–Wagner polarization and multiple scattering effects. In addition, effective impedance matching can be achieved by incorporating $CuFe_2O_4$ nanoparticles into conductive networks based on carbon materials or polymers, enabling simultaneous tuning of permittivity and permeability and thereby favoring absorption-dominated shielding over pure reflection.

A notable demonstration is $CuFe_2O_4$-loaded brick (10 wt% filler), where the composite exhibited strong microwave absorption with RL ≈ 58.54 dB, EAB ≈ 4.22 GHz (RL > 10 dB) at 2.5 mm thickness, and reported shielding of >58% of incident waves in X-band at relatively low loading. The authors attribute performance to combined conductive loss, hopping conduction, magnetic resonance processes, relaxation loss, and "secondary field" effects, highlighting absorption-dominant behavior [90].

In polymer matrices, ferrite-only formulations often provide modest-to-moderate SE, primarily through absorption contributions. For example, LDPE composites filled with $CuFe_2O_4$ have been reported to increase total SE compared with neat LDPE (values reported around ~11–13 dB depending on formulation/processing), reflecting the limited conductivity of the polymer–ferrite system without an additional conductive network [91].

$CuFe_2O_4$ is frequently integrated with 2D or conductive phases to increase attenuation constant and broaden bandwidth. For example, CuFe2O4/MoS2 composites have been widely cited as efficient microwave attenuators due to improved impedance matching and synergistic dielectric–magnetic loss pathways [92].

Similarly, metal–ferrite designs (e.g., Co@ $CuFe_2O_4$) have been reported with strong RL minima and broad bandwidth, typically rationalized by combined conductive pathways, polarization losses, and multiple scattering within hierarchical microstructures [93].

Design rules that consistently improve EMI shielding performance in $CuFe_2O_4$-based systems emphasize the importance of transitioning from ferrite-only formulations to hybrid architectures. The incorporation of $CuFe_2O_4$ with conductive phases such as reduced graphene oxide, carbon nanotubes, carbon black, or conductive polymers enables the simultaneous enhancement of electromagnetic attenuation and impedance matching, which is essential for achieving absorption-dominant shielding [86, 87].

In parallel, deliberate control of interfacial structures through core–shell configurations, surface functionalization, and heterojunction engineering promotes interfacial polarization and inhibits nanoparticle agglomeration, thereby improving frequency stability and broadband performance [86, 92]. Optimization of composite thickness and filler loading represents another critical factor, as maximum absorption is attained only under appropriate impedance-matching conditions. Excessive conductive content may deteriorate matching characteristics and shift the shielding mechanism toward undesirable reflection-dominated behavior [86, 90]. Finally, the design of absorption-oriented shielding materials is increasingly prioritized in view of sustainability and device safety considerations, since absorber-type shields minimize secondary electromagnetic pollution caused by reflected waves and are consistent with emerging trends in next-generation EMI mitigation technologies [88, 90].

Key open issues include: (i) reproducible control of cation distribution/defects, which strongly affects μ, ε, and relaxation behavior; (ii) limited comparability across studies due to different frequency windows (RF vs X/Ku band), sample geometries, and reporting conventions; and (iii) scale-up constraints when sophisticated heterostructures are required for top-tier performance. Broad EMI reviews increasingly call for standardized reporting and structure–property models (linking microstructure → ε/μ spectra → SE/RL), which is especially relevant for ferrite-based absorptive shields [86, 87].

2.5. Functional Sensing Platforms Based on $CuFe_2O_4$ Nanoparticles

Copper ferrite ($CuFe_2O_4$) nanoparticles have attracted research interest as functional sensing materials due to their semiconducting behavior, magnetic properties, and high surface reactivity that facilitate interaction with target analytes. One of the earliest demonstrations of $CuFe_2O_4$ in sensing was in conductometric gas sensors, where nanocrystalline $CuFe_2O_4$ thick films exhibited measurable conductance changes upon exposure to reducing gases such as ammonia (NH3), acetone, hydrogen (H2), and ethanol, showing rapid response and recovery characteristics that are important for practical gas detection devices [94]. Moreover, $CuFe_2O_4$ nanoparticles fabricated into pressed disk conductometric sensors demonstrated sensitivity and selectivity toward hydrogen sulfide (H_2S) gas at concentrations as low as tens of parts per million, illustrating intrinsic gas-sensing potential arising from surface adsorption–desorption processes and the associated modulation of electrical resistance [95].

Beyond simple gas chemiresistors, recent advances include the development of $CuFe_2O_4$-based composite sensing platforms where incorporation with other materials enhances performance metrics. For example, modified electrodes using lanthanum-doped $CuFe_2O_4$ nanomaterials combined with conductive graphite powder have been investigated for electrochemical sensing of heavy metal ions (e.g., lead) and pharmaceutical molecules such as paracetamol, showing admirable sensitivity and low over-voltage requirements [76]. In addition, composite sensing films where $CuFe_2O_4$ is integrated with heterostructure elements or reduced graphene oxide (rGO) facilitate improved electron transfer and increased active surface area, which can substantially improve the response to target analytes in chemiresistive and electrochemical sensor configurations [96].

The sensing performance of $CuFe_2O_4$-based platforms is strongly influenced by the nanoparticle synthesis method, particle size, crystallinity, and surface chemistry, all of which determine the density of active sites and charge transfer pathways available for analyte interaction [97]. As research progresses, integrating $CuFe_2O_4$ nanoparticles into micro- and nanoelectronic sensor architectures holds promise for sensitive, selective, and potentially low-cost detection of gases, biomolecules, and environmental contaminants.

III. Challenges, Recovery, and Reusability

The economic and practical viability of $CuFe_2O_4$-based functional materials is strongly dependent on material cost, recovery efficiency, long-term stability, and versatility across multiple application domains. Catalytic and functional systems that rely on complex fabrication routes or expensive components often impose significant financial and environmental constraints, thereby limiting their large-scale implementation. In this context, the development of low-cost, recyclable, and multifunctional nanomaterials remains a central objective for sustainable technologies.

$CuFe_2O_4$ nanoparticles offer distinct advantages due to their superparamagnetic behavior, which enables rapid and selective separation from liquid media using external magnetic fields. Magnetic recovery is considerably more efficient than conventional separation techniques such as filtration or centrifugation, while minimizing material loss and secondary contamination. This feature is particularly valuable for photocatalytic and adsorption-based water treatment systems, as well as for reusable sensing platforms operating in aqueous environments.

The magnetic recoverability of $CuFe_2O_4$ contributes to its classification as a sustainable heterogeneous catalyst and functional material. Numerous studies report that $CuFe_2O_4$-based systems retain a substantial fraction of their activity over repeated operation cycles. For instance, Verghese et al. [160] reported approximately 60% retention of dye removal efficiency after four adsorption cycles. In general, $CuFe_2O_4$ materials preserve acceptable photocatalytic and adsorptive performance for three to five reuse cycles, depending on synthesis conditions, surface modification, and operating parameters [94,110,160]. Similar stability trends have been observed in EMI shielding composites and sensing platforms, where mechanical integrity, interfacial stability, and resistance to environmental degradation play crucial roles in long-term performance.

Despite these advantages, gradual degradation is frequently observed during extended use. In catalytic systems, activity loss is commonly associated with surface fouling, partial leaching of active species, and nanoparticle agglomeration. In EMI shielding and sensing devices, performance deterioration may result from filler dispersion instability, interface degradation, oxidation, or irreversible surface reactions with analytes. These challenges highlight the need for effective regeneration and stabilization strategies, including thermal treatment, chemical washing, surface refunctionalization, encapsulation, and composite structure optimization.

Overall, the combination of low material cost, chemical robustness, magnetic recoverability, and multifunctionality makes $CuFe_2O_4$ nanoparticles attractive candidates for integrated environmental, electronic, and sensing technologies. Beyond water purification, their demonstrated potential in electromagnetic interference shielding and chemical sensing expands their relevance to advanced communication systems, smart devices, and environmental monitoring platforms. Future research should focus on elucidating degradation mechanisms under realistic operating conditions, establishing standardized lifetime evaluation protocols, and developing predictive design frameworks that couple catalytic, electromagnetic, and sensing functionalities to enable reliable large-scale deployment.

Conclusions and prospects

This review has highlighted the versatility of $CuFe_2O_4$ nanoparticles and their nanocomposites in terms of synthesis strategies, structure–property relationships, and multifunctional applications, with particular emphasis on wastewater remediation, electromagnetic interference shielding, and sensing technologies. The physicochemical, magnetic, electrical, and surface properties of $CuFe_2O_4$ can be effectively tailored through careful selection of synthesis routes, including sol–gel, hydrothermal, combustion-based, and mechanochemical methods. Key processing parameters such as pH, calcination temperature, precursor stoichiometry, dopant incorporation, and post-treatment conditions govern crystallite size, morphology, phase stability, saturation magnetization, coercivity, dielectric response, and surface reactivity, thereby determining overall functional performance.

The superparamagnetic behavior of $CuFe_2O_4$ nanoparticles, typically achieved at particle sizes below approximately 30 nm, represents a major advantage for practical implementation. This feature enables rapid magnetic recovery and reuse of catalysts, adsorbents, and sensing elements using external magnetic fields, eliminating the need for energy-intensive separation processes. Consequently, $CuFe_2O_4$-based materials are particularly attractive for sustainable water treatment systems and reusable sensing platforms operating in complex aqueous environments.

Considerable efforts have been devoted to enhancing magnetic, dielectric, and electronic properties through cation substitution and composite engineering. However, reported trends in saturation magnetization, coercivity, permittivity, and attenuation behavior are frequently non-linear, indicating that dopant and filler selection remains largely empirical. Future progress requires a rational design framework that integrates ionic radius, valence state, site occupancy, and defect chemistry. In this context, computational approaches such as density functional theory, molecular dynamics simulations, and electromagnetic modeling are expected to play an seevital role in predicting optimal compositions, heterointerfaces, and microstructures for catalytic, shielding, and sensing applications.

From a photocatalytic perspective, $CuFe_2O_4$ exhibits strong visible-light activity owing to its narrow band gap (approximately 1.7–1.9 eV) and the presence of Fe^{3+}/Fe^{2+} and Cu^{2+}/Cu^{+} redox couples. While rare-earth doping and surface modification have shown potential for suppressing charge-carrier recombination, future photocatalyst design should emphasize rational heterostructure engineering, optimized band alignment, interfacial charge transfer, and synergistic dielectric–magnetic effects. Similar design principles are relevant for EMI shielding and microwave absorption systems, where impedance matching, interfacial polarization, and loss mechanisms must be simultaneously optimized.

Despite substantial progress, the application of $CuFe_2O_4$ nanoparticles for the removal and detection of complex and emerging contaminants, including pharmaceutical residues, endocrine-disrupting compounds, pesticides, and microplastics, remains relatively underexplored. In parallel, long-term stability, environmental durability, and performance retention of $CuFe_2O_4$-based EMI shields and sensor devices under realistic operating conditions require more systematic investigation. Studies conducted in real wastewater matrices, variable humidity environments, and mechanically stressed composites are particularly needed to assess practical reliability.

$CuFe_2O_4$ nanoparticles and their composites represent a promising class of multifunctional materials that combine low toxicity, environmental compatibility, magnetic separability, visible-light-driven photocatalytic activity, electromagnetic attenuation capability, and sensing functionality. Their scalable synthesis, recyclability, and adaptability to hybrid architectures position $CuFe_2O_4$ as strong candidates for integration into next-generation water treatment systems, smart sensing platforms, and electromagnetic protection technologies. Continued integration of theoretical modeling, advanced characterization, standardized lifetime testing, and pilot-scale validation will be essential to fully realize the potential of $CuFe_2O_4$-based materials in addressing interconnected environmental, technological, and sustainability challenges.

Funding: *This work was supported by the Ministry of Education and Science of Ukraine [grant number 24BF051-01M (0124U001654)].*

Acknowledgments: *J. Mazurenko acknowledges the Ministry of Education and Science of Ukraine for funding the project 24BF051-01M (0124U001654).*

MazurenkoYuliia – Candidate of Physical and Mathematical Sciences (Ph.D.), Research Scientist at Laboratory for Physics of Magnetic Films, G.V. Kurdyumov Institute for Metal Physics, N.A.S. of Ukraine;

Turovska Liliia – Candidate of Chemical Sciences (Ph.D), Vice-Rector for Research and International Affairs, Vasyl Stefanyk Carpathian National University;

Mokliak Mariia – PhD Student, Department of Applied Physics and Materials Science, Vasyl Stefanyk Precarpathian National University;

Kaykan Larysa – Doctor of Physical and Mathematical Sciences, Senior Researcher, Leading Research Scientist at the Laboratory for Physics of Magnetic Films, G.V. Kurdyumov Institute for Metal Physics, N.A.S. of Ukraine.

Mokliak Volodymyr – Doctor of Physical and Mathematical Sciences, Professor, Head of Laboratory for Physics of Magnetic Films, G.V. Kurdyumov Institute for Metal Physics, N.A.S. of Ukraine, Professor of the Department of Physical and Mathematical Sciences, Ivano-Frankivsk National Technical University of Oil and Gas.

[1] P.J. van der Zaag, *Ferrites*, Encyclopedia of Materials: Science and Technology, 3033 (2001); https://doi.org/10.1016/b0–08–043152–6/00542–8.

[2] S.R. Daf et al., *Effects of synthesis methods on the structural and magnetic properties of Mg0.2Ni0.6Zn0.2Fe2O4 spinel ferrite*, Journal of Crystal Growth, 660, 128157 (2025); https://doi.org/10.1016/j.jcrysgro.2025.128157.

[3] B. Süngü Mısırlıoğlu et al., *Enhanced dielectric properties of copper substituted nickel ferrite nanoparticles for energy storage applications,* Journal of Physics and Chemistry of Solids, 193, 112195 (2024); https://doi.org/10.1016/j.jpcs.2024.112195.

[4] A. A. Shati et al., *Functionalization of porous silica with graphene oxide and polyethyleneimine, containing zinc copper ferrite nanoparticles for water treatment and antibacterial application*, Environmental Pollution, 348, 123745 (2024); https://doi.org/10.1016/j.envpol.2024.123745.

[5] V. L. Savithri Vatsalya et al., *Studies on nano crystalline copper doped Nickel Zinc ferrites for optoelectronic applications*, Journal of Luminescence, 252, 119314 (2022); https://doi.org/10.1016/j.jlumin.2022.119314.

[6] X. Qian et al., *Unlocking the value of Copper and Aluminum Foils from Spent Lithium–ion Batteries*, Energy Storage Materials, 104309 (2025); https://doi.org/10.1016/j.ensm.2025.104309.

[7] N. Alghamdi et al., *Structural, magnetic and toxicity studies of ferrite particles employed as contrast agents for magnetic resonance imaging thermometry*, Journal of Magnetism and Magnetic Materials, 497, 165981 (2020); https://doi.org/10.1016/j.jmmm.2019.165981.

[8] M.A. A. El–Khair et al., *Harvesting the synergistic effect of CuFe2O4@Ni–MOF nanomagnetic photocatalyst for enhanced visible light–driven green hydrogen production*, International Journal of Hydrogen Energy, 101, 280 – 294 (2025); https://doi.org/10.1016/j.ijhydene.2024.12.449.

[9] J.C. Navarro et al., *Spinel ferrite catalysts for CO2 reduction via reverse water gas shift reaction*, Journal of CO2 Utilization, 68, 102356 (2023); https://doi.org/10.1016/j.jcou.2022.102356.

[10] S. Bhagat et al., *Harnessing synergy: Immobilized Cu(II) and Pd(II) species on magnetic silica–coated copper ferrite for A3 and Sonogashira coupling reactions,* Applied Surface Science, 687, 162264 (2025); https://doi.org/10.1016/j.apsusc.2024.162264.

[11] T. Wang et al., *In–situ surface reconstruction of BiVO4/CuFe2O4 photoanode for efficient and robust solar water oxidation*, Chemical Engineering Journal, 509, 161333 (2025); https://doi.org/10.1016/j.cej.2025.161333.

[12] K. S. Muthuvelu et al., *A novel method for improving laccase activity by immobilization onto copper ferrite nanoparticles for lignin degradation*, International Journal of Biological Macromolecules, 152, 1098 (2020); https://doi.org/10.1016/j.ijbiomac.2019.10.198.

[13] C. Zhu et al., *Fabrication of temozolomide–loaded polydopamine–coated copper ferrite clocked bovine serum albumin nanoparticles delivery for glioma cancer and induction of apoptosis mechanism*, Journal of Drug Delivery Science and Technology, 106, 106642 (2025); https://doi.org/10.1016/j.jddst.2025.106642.

[14] M. Ismael, M. Wark, *A simple sol – gel method for the synthesis of Pt co–catalyzed spinel–type CuFe2O4 for hydrogen production; the role of crystallinity and band gap energy*, Fuel, 359, 130429 (2024); https://doi.org/10.1016/j.fuel.2023.130429.

[15] M. P. Ghosh et al., *Copper doped nickel ferrite nanoparticles: Jahn–Teller distortion and its effect on microstructural, magnetic and electronic properties*, Materials Science and Engineering: B, 263, 114864 (2021); https://doi.org/10.1016/j.mseb.2020.114864.

[16] A. Kyono et al., *High–pressure behavior of cuprospinel CuFe2O4: Influence of the Jahn–Teller effect on the spinel structure*, American Mineralogist, 100(8 – 9), 1752 (2015); https://doi.org/10.2138/am–2015–5224.

[17] I. Nedkov et al., *Magnetic structure and collective Jahn – Teller distortions in nanostructured particles of CuFe2O4*, Applied Surface Science, 253(5), 2589 (2006); https://doi.org/10.1016/j.apsusc.2006.05.049.

[18] E. Kester et al., *Valence states of copper in copper ferrite spinels CuxFe3−xO4 (0 < x ≤ 1) fine powders: Evidence of copper insertion*, Thermochimica Acta, 297(1 – 2), 71 (1997); https://doi.org/10.1016/s0040–6031(97)00123–8.

[19] J. Z. Jiang et al., *Magnetic properties of nanostructured CuFe2O4*, Journal of Physics: Condensed Matter, 11(20), 4063 (1999); https://doi.org/10.1088/0953–8984/11/20/313.

[20] M. M. Rashad et al., *Magnetic and catalytic properties of cubic copper ferrite nanopowders synthesized from secondary resources*, Advanced Powder Technology, 23(3), 315 (2012); https://doi.org/10.1016/j.apt.2011.04.005.

[21] *E. E. Ateia et al., Novelty* characterization and enhancement of magnetic properties of Co and Cu nanoferrites, Journal of Materials Science: Materials in Electronics, 28(1), 241 (2016); https://doi.org/10.1007/s10854–016–5517–y.

[22] M. Rahimi–Nasrabadi et al., *Nanocrystalline Ce–doped copper ferrite: synthesis, characterization, and its photocatalyst application*, Journal of Materials Science: Materials in Electronics, 27(11), 11691 (2016); https://doi.org/10.1007/s10854–016–5305–8.

[23] A. R. Chavan et al., *Effect of Zr4+ dopants on micro-structural and antibacterial characteristics of CuFe2O4 nanoparticles produced via sol-gel auto combustion*, Journal of Sol-Gel Science and Technology, 116, 434 (2025); https://doi.org/10.1007/s10971-025-06730-8.

[24] L. Khanna et al., *Effect of size and silica coating on structural, magnetic as well as cytotoxicity properties of copper ferrite nanoparticles*, Materials Science and Engineering*:* C, 97, 552 (2019); https://doi.org/10.1016/j.msec.2018.12.051.

[25] L. B. Zakiyah et al., *Up–scalable synthesis of size–controlled copper ferrite nanocrystals by thermal treatment method*, Materials Science in Semiconductor Processing, 40, 564 (2015); https://doi.org/10.1016/j.mssp.2015.07.027.

[26] M. Á. Cobos et al., *Ball milling and annealing effect in structural and magnetic properties of copper ferrite by ceramic synthesis,* Journal of Alloys and Compounds, 1006, 176206 (2024); https://doi.org/10.1016/j.jallcom.2024.176206.

[27] J. Mazurenko et al., *Inductive Heating Behavior of Copper Ferrite Magnetic Nanoparticles*, Physics and Chemistry of Solid State, 26(2), 312 (2025); https://doi.org/10.15330/pcss.26.2.312-321.

[28] M.M. Rashad et al., *Investigation of the structural, optical and magnetic properties of CuO/CuFe2O4 nanocomposites synthesized via simple microemulsion method*, Ceramics International, 41(9), 12237 (2015); https://doi.org/10.1016/j.ceramint.2015.06.046.

[29] *J. E. Tasca et al., Preparation and characterization of CuFe2O4 bulk catalysts,* Ceramics International, 37(3), 803 (2011); https://doi.org/10.1016/j.ceramint.2010.10.023.

[30] T. G. Altincekic et al., Synthesis and characterization of CuFe2O4 nanorods synthesized by polyol route, Journal of Alloys and Compounds, 493(1 – 2), 493 (2010); https://doi.org/10.1016/j.jallcom.2009.12.140.

[31] F. S. M. Sinfrônio et al., *Effect of Co–substitution on the Vibrational, Magnetic, and Dielectric Properties of Copper Ferrites Obtained by Microwave–Assisted Hydrothermal Method*, Journal of Electronic Materials, 47(11), 6821 (2018); https://doi.org/10.1007/s11664–018–6598–6.

[32] E. Manova et al., *Nanosized copper ferrite materials: Mechanochemical synthesis and characterization*, Journal of Solid State Chemistry, 184(5), 1153 (2011); https://doi.org/10.1016/j.jssc.2011.03.035.

[33] P. Thakur et al., *A review on MnZn ferrites: Synthesis, characterization and applications*, Ceramics International, 46(10), 15740 (2020); https://doi.org/10.1016/j.ceramint.2020.03.287.

[34] C. Sedrati et al., *Structure and magnetic properties of nickel ferrites* synthesized by a facile co–precipitation method: effect of the Fe/Ni ratio, Journal *of Materials Science: Materials in Electronics*, 32(19), 24548 (2021); https://doi.org/10.1007/s10854–021–06932–0.

[35] Y. Peng et al., *Effect of reaction condition on microstructure and properties of (NiCuZn)Fe2O4 nanoparticles synthesized via co–precipitation with ultrasonic irradiation*, Ultrasonics Sonochemistry, 71, 105369 (2021); https://doi.org/10.1016/j.ultsonch.2020.105369.

[36] C. R. Kalaiselvan et al., *Manganese ferrite (MnFe2O4) nanostructures for cancer theranostics*, Coordination Chemistry Reviews, 473, 214809 (2022); https://doi.org/10.1016/j.ccr.2022.214809.

[37] S. Liu et al., *Preparation, surface functionalization and application of Fe3O4 magnetic nanoparticles*, Advances in Colloid and Interface Science, 281, 102165 (2020); https://doi.org/10.1016/j.cis.2020.102165.

[38] M. R. Zamani Kouhpanji, B. J. H. Stadler, *A Guideline for Effectively Synthesizing and Characterizing Magnetic Nanoparticles for Advancing Nanobiotechnology: A Review*, Sensors, 20(9), 2554 (2020); https://doi.org/10.3390/s20092554.

[39] G. Rana et al., *Recent advances on nickel nano–ferrite: A review on processing techniques, properties and diverse applications,* Chemical Engineering Research and Design, 175, 182 (2021); https://doi.org/10.1016/j.cherd.2021.08.040.

[40] M. Vishwas et al., *Synthesis, characterization and photo–catalytic activity of magnetic CoFe2O4 nanoparticles prepared by temperature controlled co–precipitation method*, Materials Today: Proceedings, 68, 497 (2022); https://doi.org/10.1016/j.matpr.2022.07.429.

[41] B. Paz-Díaz et al., *ZnFe2O4 and CuFe2O4 Nanocrystals: Synthesis, Characterization, and Bactericidal Application*, Journal of Cluster Science, 34(1), 111 (2021); https://doi.org/10.1007/s10876-021-02203-4.

[42] M. Weißpflog et al., *Non–Stoichiometric Cobalt Ferrite Nanoparticles by Green Hydrothermal Synthesis and their Potential for Hyperthermia Applications, The Journal of Physical Chemistry C*, 128(37), 15598 – 15612 (2024); https://doi.org/10.1021/acs.jpcc.4c03589.

[43] R. S. Melo et al., *Hydrothermal synthesis of nickel doped cobalt ferrite nanoparticles: optical and magnetic properties,* Journal of Materials Science: Materials in Electronics, 29(17), 14657 (2018); https://doi.org/10.1007/s10854–018–9602–2.

[44] M. Hatefi et al., *Evaluation of the impact of hydrothermal synthesis parameters of CuFe2O4/CeO2-MgO catalysts in water-gas shift reaction*, Chemical Engineering Research and Design, 218, 350 (2025); https://doi.org/10.1016/j.cherd.2025.05.004.

[45] A. Zeleňáková et al., *Cobalt-ferrite nano-cubes for magnetic hyperthermia applications*, Journal of Alloys and Compounds, 989, 174415 (2024); https://doi.org/10.1016/j.jallcom.2024.174415.

[46] M. Hodlevska et al., *Hydrothermally synthesized NiFe2O4/rGO composites: structure, morphology and electrical conductivity,* Applied Nanoscience, 13(7), 5199 (2023); https://doi.org/10.1007/s13204-022-02741-x.

[47] F. Majid et al., *Effect of Hydrothermal Reaction Time on Electrical, Structural and Magnetic Properties of Cobalt Ferrite,* Zeitschrift Für Physikalische Chemie, 234(2), 323 (2019); https://doi.org/10.1515/zpch-2019-1423.

[48] S. Sheshmani, N. Mohammad Hosseini, *Engineered Heterostructure Photocatalyst: Chitosan-Coated Chromium Ferrite/Graphite Oxide Synthesized Hydrothermally for Environmental Remediation*, Journal of Polymers and the Environment, 33(2), 794 (2024); https://doi.org/10.1007/s10924-024-03433-z.

[49] L. S. Kaykan et al., *Effect of Nickel Ions Substitution on the Structural and Electrical Properties of a Nanosized Lithium-iron Ferrite Obtained by the Sol-gel Auto-combustion Method*, Journal of Nano- and Electronic Physics, 11(5), 05041 (2019); https://doi.org/10.21272/jnep.11(5).05041.

[50] B. K. Ostafiychuk et al., *Effect of substitution on the mechanism of conductivity of ultra dispersed lithium - iron spinel, substituted with magnesium ions*, Journal of Nano- and Electronic Physics, 9(5), 05018 (2017); https://doi.org/10.21272/jnep.9(5).05018.

[51] J. Mazurenko et al., *Optimizing the structural,* morphological, and dielectric properties of copper ferrite through magnesium substitution, Applied *Physics A*, 131(9), (2025); https://doi.org/10.1007/s00339-025-08741-2.

[52] J. Mazurenko et al., *Enhanced Synthesis of Copper Ferrite Magnetic Nanoparticles via Polymer-Assisted Sol-Gel Autocombustion Method for Magnetic Hyperthermia Applications*, Journal of Nano Research, 84, 95 (2024); https://doi.org/10.4028/p-jbv1le.

[53] N. Sanpo, *Solution Precursor Plasma Spray System*, SpringerBriefs in Materials, 1, 3 (2014); https://doi.org/10.1007/978–3–319–07025–4_1.

[54] S. Kanagesan et al., *Evaluation of Antioxidant and Cytotoxicity Activities of Copper Ferrite (CuFe2O4) and Zinc Ferrite (ZnFe2O4) Nanoparticles Synthesized by Sol–Gel Self–Combustion Method*, Applied Sciences, 6(9), 184 (2016); https://doi.org/10.3390/app6090184.

[55] T. P. Oliveira et al., *Synthesis, Characterization, and Photocatalytic Investigation of CuFe2O4 for the Degradation of Dyes under Visible Light*, Catalysts, 12(6), 623 (2022); https://doi.org/10.3390/catal12060623.

[56] I. G. Jhala et al., *Structural and magnetic properties of cobalt ferrite nanoparticles synthesized by auto–combustion sol–gel method*, Next Materials, 9, 101120 (2025); https://doi.org/10.1016/j.nxmate.2025.101120.

[57] M. S. Al Maashani et al., *The structural and magnetic properties of the nano-CoFe2O4 ferrite prepared by sol-gel auto-combustion technique,* Journal of Alloys and Compounds, 817, 152786 (2020); https://doi.org/10.1016/j.jallcom.2019.152786.

[58] M. H. Nasr et al., *Synthesis, structural, electrical and magnetic characteristics of Co–Cd spinel nano ferrites synthesized via sol-gel auto combustion method*, Journal of Sol-Gel Science and Technology, 116(1), 34 (2024); https://doi.org/10.1007/s10971-024-06327-7.

[59] R. Dudhal et al., *Role of pH on the Structural and Infrared Properties of Nickel Ferrite Nanoparticles Prepared via Sol-Gel Auto Combustion Method*, Advanced Materials Research, 1169, 15 (2022); https://doi.org/10.4028/p-1pbj14.

[60] R. B. Sathe et al., *Studies on sol–gel autocombustion processed Ni–Zn–Mg ferrite system: effect of calcination temperature, thermoelectric power, and gas sensing application*, Journal of Materials Science: Materials in Electronics, 35(27), (2024); https://doi.org/10.1007/s10854-024-13466-8.

[61] S. V. Bhandare et al., *Annealing temperature dependent structural and magnetic properties of MnFe2O4 nanoparticles grown by sol-gel auto-combustion method*, Journal of Magnetism and Magnetic Materials, 433, 29 (2017); https://doi.org/10.1016/j.jmmm.2017.02.040.

[62] V.D. Phung et al., *Co-precipitated synthesis of CuFe2O4/CuO composite: A promising anode material for high-performance lithium-ion batteries*, Ceramics International, (2025); https://doi.org/10.1016/j.ceramint.2025.07.040.

[63] K. Razzaq et al., *Improvement in catalytic performance of CuFe2O4/PANI nanocomposite for robust water splitting*, Electrochimica Acta, 537, 146810 (2025); https://doi.org/10.1016/j.electacta.2025.146810.

[64] Y. Hong et al., *Effects of the phase transition on the photoelectrochemical properties of CuFe2O4 composite photoelectrode*, Optik, 318, 172095 (2024); https://doi.org/10.1016/j.ijleo.2024.172095.

[65] M. Mokliak et al., *Influence of Neodymium Doping on the Thermomagnetic Response and Colloidal Behavior of Copper Ferrite Nanoparticles*, Physics and Chemistry of Solid State, 26(3), 564 (2025); https://doi.org/10.15330/pcss.26.3.564-577.

[66] F. Heydari et al., *Solvothermal synthesis of polyvinyl pyrrolidone encapsulated, amine-functionalized copper ferrite and its use as a magnetic resonance imaging contrast agent*, PLOS ONE, 20(2), e0316221 (2025); https://doi.org/10.1371/journal.pone.0316221.

[67] *H. Lahmar et al., Photocatalytic Evolution of Hydrogen on CuFe2O4, Springer Proceedings in Energy*, 129 – 136 (2020); https://doi.org/10.1007/978-981-15-6595-3_18.

[68] J. Mazurenko et al., *Photocatalytic efficiency of nickel-doped copper ferrite in organic dye decomposition*, Nano-Structures & Nano-Objects, 45, 101603 (2026); https://doi.org/10.1016/j.nanoso.2025.101603.

[69] A. Akbar et al., *Magnetically recoverable biogenic CuFe2O4 nanoparticles for sustainable catalytic degradation of organic dyes*, Journal of Water Process Engineering, 79, 108871 (2025); https://doi.org/10.1016/j.jwpe.2025.108871.

[70] Z. Irshad et al., *Phyto-mechanochemical Synthesis of Copper Ferrite Nanoparticles: Structural, Magnetic, Photocatalytic, and Antibacterial Properties*, ChemistrySelect, 10(8), (2025); https://doi.org/10.1002/slct.202405145.

[71] M. Kamel Attar Kar et al., *Structural, Optical, and Isothermic Studies of CuFe2O4 and Zn-Doped CuFe2O4 Nanoferrite as a Magnetic Catalyst for Photocatalytic Degradation of Direct Red 264 Under Visible Light Irradiation*, Environmental Progress & Sustainable Energy, 38(4), (2019); https://doi.org/10.1002/ep.13109.

[72] N. M. Patil et al., *Synthesis of CuFe2O4 Nanoparticles for Applications in Biodiesel Production and Degradation of Methylene Blue Dye*, Iranian Journal of Catalysis, 15(3), (2025); https://doi.org/10.57647/j.ijc.2025.1503.32.

[73] D. Zala, A. Ray, *Synthetically modified mixed phase inverse spinel CuFe$_2$O$_4$ magnetic nanoparticles: Structure, physical, and electrochemical properties for photocatalytic applications*, Physica B: Condensed Matter, 699, 416770 (2025); https://doi.org/10.1016/j.physb.2024.416770.

[74] M. Giridhar et al., *Sustainable approach of La doped CuFe$_2$O$_4$ nanomaterial for electrochemical lead and paracetamol sensing action with multiple applications*, Scientific Reports, 13(1), (2023); https://doi.org/10.1038/s41598-023-45029-y.

[75] S. Tahir et al., *The synergistic effect of g-C3N$_4$/GO/CuFe$_2$O$_4$ for efficient sunlight-driven photocatalytic degradation of methylene blue*, International Journal of Environmental Science and Technology, 22(6), 4829 (2024); https://doi.org/10.1007/s13762-024-05929-6.

[76] Y. Lin et al., *Catalytic reduction of p-nitrophenol by g-C3N$_4$/CuFe$_2$O$_4$ magnetic nanocomposites*, Optical Materials, 157, 116070 (2024); https://doi.org/10.1016/j.optmat.2024.116070.

[77] E. A. Afshar, M. A. Taher, *New fabrication of CuFe$_2$O$_4$/PAMAM nanocomposites by an efficient removal performance for organic dyes: Kinetic study*, Environmental Research, 204, 112048 (2022); https://doi.org/10.1016/j.envres.2021.112048.

[78] S. Hassan et al., *CuFe$_2$O$_4$/Polyaniline (PANI) Nanocomposite for the Hazard Mercuric Ion Removal: Synthesis, Characterization, and Adsorption Properties Study*, Molecules, 25(12), 2721 (2020); https://doi.org/10.3390/molecules25122721.

[79] I. Othman et al., *Facile Preparation of Magnetic CuFe$_2$O$_4$ on Sepiolite/GO Nanocomposites for Efficient Removal of Pb(II) and Cd(II) from Aqueous Solution*, ACS Omega, 8(42), 38828 (2023); https://doi.org/10.1021/acsomega.3c02006.

[80] A. H. Kamel et al., *Synthesis and Characterization of CuFe$_2$O$_4$ Nanoparticles Modified with Polythiophene: Applications to Mercuric Ions Removal*, Nanomaterials, 10(3), 586 (2020); https://doi.org/10.3390/nano10030586.

[81] R. Ramadan, M. M. El-Masry, *Effect of (Co and Zn) doping on structural, characterization and the heavy metal removal efficiency of CuFe$_2$O$_4$ nanoparticles*, Journal of the Australian Ceramic Society, 60(2), 509 (2023); https://doi.org/10.1007/s41779-023-00932-5.

[82] Y. Xia et al., *Magnetically separable CuFe$_2$O4/ZnIn$_2$S$_4$ heterojunction photocatalyst for simultaneous removal of Cr(VI) and CIP*, Journal of Cleaner Production, 434, 140445 (2024); https://doi.org/10.1016/j.jclepro.2023.140445.

[83] K. Derkaoui et al., *Spinel ferrites MFe$_2$O4 (M = Cu, Ni, Mn) as noble-metal-free electrocatalysts for hydrogen evolution: Highlighting the superior activity of CuFe$_2$O$_4$*, Journal of the Indian Chemical Society, 102(12), 102234 (2025); https://doi.org/10.1016/j.jics.2025.102234.

[84] C. Van Tran et al., *Self-assembly of porphyrin nanofiber on the surface CuFe$_2$O$_4$ nanoparticles: A novel photoanode for enhanced photo-electrochemical water splitting*, Fuel, 380, 133196 (2025); https://doi.org/10.1016/j.fuel.2024.133196.

[85] Z. Lin et al., *In situ construction of CuFe$_2$O$_4$/CuO heterojunction photocathode for improved solar water splitting,* Journal of Alloys and Compounds, 1042, 184174 (2025); https://doi.org/10.1016/j.jallcom.2025.184174.

[86] J. T. Orasugh, S. S. Ray, *Functional and Structural Facts of Effective Electromagnetic Interference Shielding Materials: A Review*, ACS Omega, 8(9), 8134 (2023); https://doi.org/10.1021/acsomega.2c05815.

[87] S. Zecchi et al., *A Comprehensive Review of Electromagnetic Interference Shielding Composite Materials*, Micromachines, 15(2), 187 (2024); https://doi.org/10.3390/mi15020187.

[88] V. Shukla, *Review of electromagnetic interference shielding materials fabricated by iron ingredients*, Nanoscale Advances, 1(5), 1640 (2019); https://doi.org/10.1039/c9na00108e.

[89] A. Radoń et al., *Dielectric and electromagnetic interference shielding properties of high entropy (Zn,Fe,Ni,Mg,Cd)Fe$_2$O$_4$ ferrite*, Scientific Reports, 9(1), (2019); https://doi.org/10.1038/s41598-019-56586-6.

[90] S. Keykavous-Amand, R. Peymanfar, *Fabrication of clay soil/CuFe$_2$O$_4$ nanocomposite toward improving energy and shielding efficiency of buildings*, Scientific Reports, 11(1), (2021); https://doi.org/10.1038/s41598-021-00347-x.

[91] O. Yakovenko et al., *Electrodynamic properties of epoxy composites enhanced with nanosized ferrite fillers,* Ceramics International, 51(21), 34234 (2025); https://doi.org/10.1016/j.ceramint.2025.05.151.

[92] J. Liu et al., *Self-assembled MoS2/magnetic ferrite CuFe$_2$O$_4$ nanocomposite for high-efficiency microwave absorption,* Chemical Engineering Journal, 429, 132253 (2022); https://doi.org/10.1016/j.cej.2021.132253.

[93] X. Feng et al., *Innovative preparation of Co@ CuFe$_2$O$_4$ composite via ball-milling assisted chemical precipitation and annealing for glorious electromagnetic wave absorption*, International Journal of Minerals, Metallurgy and Materials, 30(3), 559 (2023); https://doi.org/10.1007/s12613-022-2488-2.

[94] Z. Sun et al., *Simple synthesis of CuFe$_2$O$_4$ nanoparticles as gas-sensing materials*, Sensors and Actuators B: Chemical, 125(1), 144 (2007); https://doi.org/10.1016/j.snb.2007.01.050.

[95] M. A. Haija et al., *Adsorption and gas sensing properties of CuFe$_2$O$_4$ nanoparticles*, Materials Science-Poland, 37(2), 289 (2019); https://doi.org/10.2478/msp-2019-0020.

[96] S. Vinothini et al., *$CuFe_2O_4$ Nanofiber Incorporated with a Three-Dimensional Graphene Sheet Composite Electrode for Supercapacitor and Electrochemical Sensor Application*, Inorganics, 12(6), 164 (2024); https://doi.org/10.3390/inorganics12060164.

[97] P. H. Phuoc et al., *Heterojunction-enhanced H2S sensing mechanism in on-chip $NiFe_2O_4$–$CuFe_2O_4$ nanofiber sensors*, Ceramics International, 52(1), 398 (2026); https://doi.org/10.1016/j.ceramint.2025.11.337.

Ю. Мазуренко[1,2,3], Л. Туровська[4], М. Мокляк[5], Л. Кайкан[1], В. Мокляк[1,6]

Синтез, проблеми та потенціал застосування наночастинок фериту міді

[1]Лабораторія фізики магнітних плівок, Інститут металофізики імені Г.В. Курдюмова НАН України, Київ, Україна;
mazurenkoyus@nas.gov.ua, kaykan@nas.gov.ua
[2]Кафедра загальної фізики, Київський національний університет імені Тараса Шевченка, Київ, Україна;
[3]Кафедра медичної інформатики, медичної та біологічної фізики, Івано-Франківський національний медичний університет, Івано-Франківськ, Україна;
[4]Кафедра менеджменту та бізнес-адміністрування, факультет менеджменту, Карпатський національний університет імені Василя Стефаника, Івано-Франківськ, Україна; liliia.turovska@cnu.edu.ua
[5]Кафедра прикладної фізики та матеріалознавства, Карпатський національний університет імені Василя Стефаника, Івано-Франківськ, Україна, mariamoklyak@gmail.com
[6]Кафедра фізико-математичних наук, Івано-Франківський національний технічний університет нафти і газу, Івано-Франківськ, Україна, volodymyr.mokliak@nung.edu.ua

Ферити – це феримагнітні матеріали на основі оксидів заліза, чиї магнітні та функціональні властивості зумовлені розподілом катіонів, наявністю дефектів та особливостями мікроструктури, що, у свою чергу, залежить від умов синтезу. Цей огляд присвячений наночастинкам шпінельного фериту міді ($CuFe_2O_4$) та аналізу того, як контрольована структура визначає його багатофункціональні характеристики.

Особливу увагу приділено питанням співіснування та стабілізації тетрагональної та кубічної фаз $CuFe_2O_4$, ролі спотворень Яна-Теллера для іонів Cu^{2+}, а також впливу кисневої нестехіометрії, перерозподілу катіонів та поверхневого розупорядкування у нанорозмірному стані. Розглянуто найбільш поширені методи хімічного синтезу – співосадження, гідротермальний/сольвотермальний методи та золь-гель синтез (зокрема шлях самопоширеного високотемпературного синтезу) – з точки зору їхньої здатності контролювати фазову чистоту, кристалічність, розмір, морфологію та хімію дефектів частинок.

Встановлено взаємозв'язок «структура-властивість» для ключових сфер застосування, розглянутих у цій роботі: фотокаталітичної деградації барвників під дією видимого світла, адсорбційного очищення від забруднювачів, фотокаталітичного виділення водню, екранування електромагнітних перешкод, поглинання мікрохвильового випромінювання та створення функціональних сенсорних платформ. Підсумовано практичні обмеження, такі як відтворюваність катіонних/дефектних станів, фазова стабільність, деградація характеристик та регенерація матеріалів. Це підкреслює необхідність розробки стандартизованих протоколів оцінки та раціонального дизайну матеріалів для створення масштабованих технологій на основі $CuFe_2O_4$ із можливістю багаторазового використання.

Ключові слова: ферити шпінелі; наночастинки мідного фериту; очищення води; фотокаталіз; екранування електромагнітних перешкод; магнітне відновлення та повторне використання; зелений синтез.